

Electrochemical Capacitance of $\text{Co}_x\text{Ni}_y\text{O}$ Preparation by Microwave-assisted Modification

Hong Wang*, Peng Wang, Zhen Yin

State Key Laboratory of Hollow Fiber Membrane Materials and Processes, School of Materials Science and Engineering, Tianjin Polytechnic University, Tianjin 300387, China.

*E-mail: waho7808@163.com

Received: 21 April 2013 / Accepted: 18 May 2013 / Published: 1 June 2013

The capacitance performance of the cobalt-doped nickel oxide ($\text{Co}_x\text{Ni}_y\text{O}$) composite electrode material made by microwave irradiation method was reported in this paper. The cobalt was doped into the $\text{Ni}(\text{OH})_2$ by ball-milling firstly, and then, the $\text{Co}_x\text{Ni}_y\text{O}$ composite electrode material was obtained by treating the doped $\text{Ni}(\text{OH})_2$ in the microwave oven at 480W for 135s. The electrochemical performances of these electrodes were investigated via cyclic voltammetry(CV) and electrochemical impedance spectroscopy (EIS) methods. The specific surface area of composite electrode material with $\text{Co/Ni}=0.4$ could be enhanced to $146.21\text{m}^2\text{g}^{-1}$, and the specific energy $61.67\text{wh}\cdot\text{kg}^{-1}$ at the current density of $200\text{mA}\cdot\text{g}^{-1}$. And also, the specific energy also remained more than 92% even after 500 charge/discharge cycles. The $\text{Co}_x\text{Ni}_y\text{O}$ composites developed by the microwave irradiation method would be excellent electrode materials for electrochemical capacitors.

Keywords: electrochemical capacitor; microwave radiation; electrode material; NiO; Co

1. INTRODUCTION

Electrochemical supercapacitor is an energy storage device based on the electrochemical reaction at the interface of electrode/electrolyte[1-4]. It has been recognized as one kind of cost-efficient energy source[5-7]. Metal oxide plays an important role in electrochemical electrode, especially for transition metal oxide due to its low cost and environment friendly characters. Metallic oxide[8-10], such as NiO, has been extensively explored as electrodes materials for electrochemical capacitor due to good cycle performance and capacitive characteristics in recent years.

It has been reported that the nanoscale NiO/Ni composite film can be prepared as electrode to fabricate the electrochemical capacitor by Liu etc.[11] The results showed that the specific capacity of these composite electrodes can be ranged from 50 to $64\text{F}\cdot\text{g}^{-1}$. Moreover, their specific energy and

power could reach 25-40 $\text{kJ}\cdot\text{kg}^{-1}$ and 4-17 $\text{kW}\cdot\text{kg}^{-1}$, respectively. All of these properties depended on the microstructure of the composite film. Liu and Anderson [12] developed the nanostructured NiO material using pyrolytic process. The electrode made by this powder had a specific capacity of $290 \text{ F}\cdot\text{g}^{-1}$ in the applied potential range of 0-0.5 V. Kyung and Kwang[13] investigated the specific capacity of NiO prepared using electrochemical deposition-thermal treatment, which could attain a maximum of $278 \text{ F}\cdot\text{g}^{-1}$.

In addition to the preparation of NiO with a higher specific surface area via various methods to enhance the capacity and cyclic performance, most studies focused on the doping modification of NiO electrode material. For example, Liu and Zhang[14] reported the NiO electrode materials by doping RuO_2 , which capacity reached $210 \text{ F}\cdot\text{g}^{-1}$ and reduced by 21% after 200 cycles. Seiji and Hiromori[15] prepared the NiO electrode material doped with polymer fibers and found that the specific capacity was $163 \text{ F}\cdot\text{g}^{-1}$. Gao et al[16] prepared uniform-structured NiO/f-MWCNTs electrode material. Under the current density of $0.20 \text{ A}\cdot\text{g}^{-1}$, the specific capacity was $384 \text{ F}\cdot\text{g}^{-1}$. The specific capacity of the activated carbon doped with nickel hydroxide could reach $314.5 \text{ F}\cdot\text{g}^{-1}$ when the content of nickel hydroxide came up to 6% in Huang's report[17]. Compared with the pure activated carbon, the specific capacity of the composite electrode materials would increase by 23.3%.

Herein, a facile and pollution free method, microwave-assisted modification, has been proposed for the fabrication of Co-doped NiO electrode material. The electrochemical performances of these doping materials were investigated via cyclic voltammetry (CV), ac impedance spectroscopy (EIS) and galvanostatic charge/discharge measurements in detail. In addition, the capacity mechanism of these doping materials had been discussed. The electrochemical performance and capacity mechanism of these electrodes were investigated in detail.

2. EXPERIMENTAL PART

2.1 Preparation of NiO with Co-doping

The $\text{NiSO}_4\cdot 6\text{H}_2\text{O}$, $\text{CoSO}_4\cdot 7\text{H}_2\text{O}$, NaOH were put in an airtight agate pot with the molar ratio of Co to Ni of 0.1~0.5. The ball milling was performed using agate balls of different sizes with the approximate mass ratio of ball to reactant of 10:1 at the speed of $300 \text{ r}\cdot\text{min}^{-1}$ of unidirectional rotation for 2 h. The products of ball milling were deposited for 6 h in water bath at 80°C and then were filtrated and washed by deionized water, ethanol and microwave dried in turn. Finally the doped $\text{Ni}(\text{OH})_2$ was finished after grinding.

Then the prepared $\text{Ni}(\text{OH})_2$ was placed in a corundum crucible, which were put into a ceramic vessel with carbon powder around the crucible. Subsequently, the ceramic vessel was moved into a microwave oven at 480 W for 135 s in air atmosphere. After the reaction, the reaction vessel was taken out and then cooled down to room temperature. Finally, the black Co-doped NiO was obtained after the reaction product was ground in an agate mortar and filtrated by 300 mesh sieves.

2.2 Preparation of electrodes and assembly of capacitors

The electrode preparation, slurry containing the prepared composite powder, acetylene black and PTFE (Poly tetra fluoro ethylene) with weight ratio of 85:5:10 and then the compound were completely dissolved in ethanol. This paste-like mixture was spread uniformly on porous nickel current collectors. After the mixture was dried at 120°C for 12 h, a 0.2mm thick film was formed under the pressure of 4 Mpa, which would be used as working electrode (anode), graphite electrode as counter electrode and reference electrode.

The cells were assembled in a glove box (dried air, moisture content < 3 ppm). The FV3 sulfonated membrane was used as separator while the LiClO₄(EC+DMC) solution as electrolyte.

2.3 Electrochemical test of Co-doped NiO electrode materials

The electrochemical measurements were carried out in a double-electrodes electrochemical cell. The asymmetry supercapacitors were characterized at room temperature by cyclic voltammetry (CV), ac impedance spectroscopy (EIS) and galvanostatic charge/discharge measurements. Galvanostatic charge/discharge behavior was performed under the conditions of constant current density of 50 mA·g⁻¹ ~ 500 mA·g⁻¹ in voltage range of 2.0~0 V with a PCBT-100 equipment. CV and EIS measurements were performed with the electrochemical workstation (Gamry Instrument model PCI4-750). CV method was carried out in the voltage range of -2~2 V. The EIS was used to explore the electrochemical behaviors of electrode materials with an amplitude of 5 mV in the frequency range of 3×10⁵~0.01 Hz. In all experiments, Co-doped NiO was the electrode material to be tested while graphite electrode was applied as the counter electrode and reference electrode, 1M LiClO₄(EC+DMC) solution as electrolyte.

2.4 Characterization of Co-doped NiO electrode materials

Synthesised products were analysed by employing X-ray powder diffractometer using CoK α to investigate the phase purity and identity of the prepared samples at scan rate of 2 θ =8°/min and scanning range from 10° to 110°. The micrograph of electrode material surface was observed by the Nova nanolab200 (FEI) Field Emission Scanning Electron Microscope (FE-SEM).

3. RESULTS AND DISCUSSION

3.1 Liquid nitrogen absorption – desorption of Co-doped NiO material

Fig.1 showed the adsorption isotherm and pore size distribution of Co-doped NiO at temperature 77K. The specific surface area (BET) and total pore volume of the doped material at the Co/Ni ratio of 0.4 were the most of 146.21 m²·g⁻¹ and 0.1982 cm³·g⁻¹, respectively. The pore sizes were mainly distributed in 1-10 nm by BJH method. Majority of the pores were meso-/macro-pores

and minority were micro-pores. The average pore size was 6.1nm. The specific surface area and total pore volume for the pure NiO material were $122.57 \text{ m}^2 \cdot \text{g}^{-1}$ and $0.1871 \text{ cm}^3 \cdot \text{g}^{-1}$, respectively. Hence, the specific surface area and total pore volume of the NiO materials after Co-doped was increased by 19.29% and 5.93%, respectively.

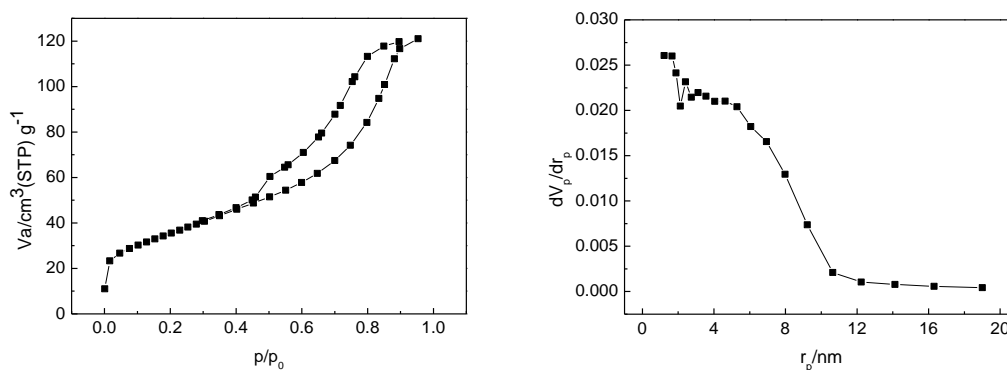


Figure 1. Nitrogen adsorption-desorption isotherm (a) and pore size distribution (b) of Co-doped NiO at temperature 77K(Co/Ni=0.4)

3.2 XRD analysis of Co-doped NiO material

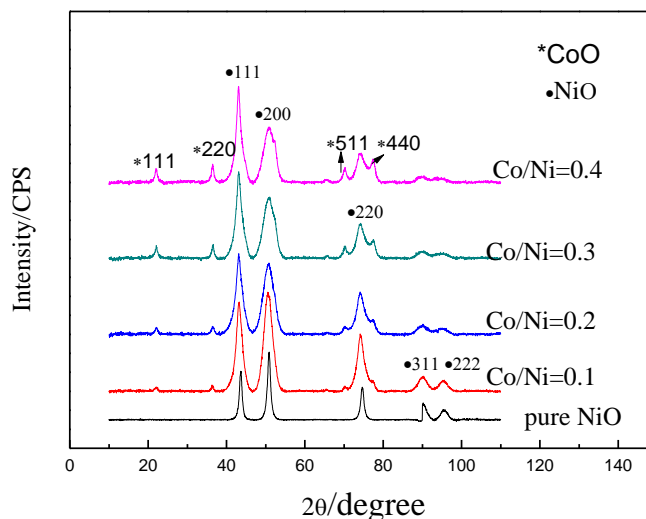


Figure 2. XRD spectra of Co-doped NiO materials.

As shown in Fig.2, the diffraction peaks at (111), (200), (220) assigned to the NiO in JCPDF(65-2901) cards. The characteristic peaks at near 22.10° , 36.47° , 70.19° and 77.50° assigned to the CoO can be distinguished after the Co doping, which indicated that Co was doped into NiO materials in the form of CoO. Moreover, the diffraction intensity of NiO peaks became weak and the full-width at half maximum width of NiO peaks wide with the increase of the Co content, which mean more lattice defects and poor crystallinity of the doped materials.

3.3 SEM analysis of Co-doped NiO material

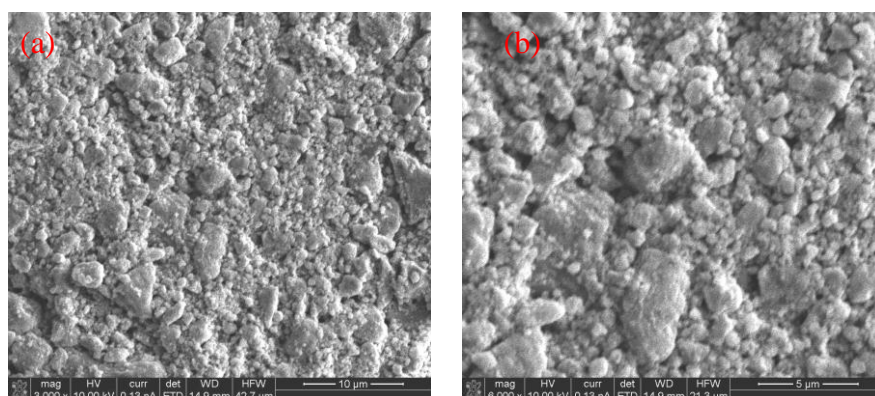


Figure 3. SEM images of Co-doped NiO material at (a) 3000 \times and (b) 6000 \times

Fig.3 showed the SEM images of Co-doped NiO material. In Fig.3a, it was observed that the surface was rough with agglomeration in part although the granules size wasn't uniform. Moreover, some bigger particles were formed due to the aggregation of primary particles, as indicated in Fig.3b.

3.4 Capacitive performance of Co-doped NiO material

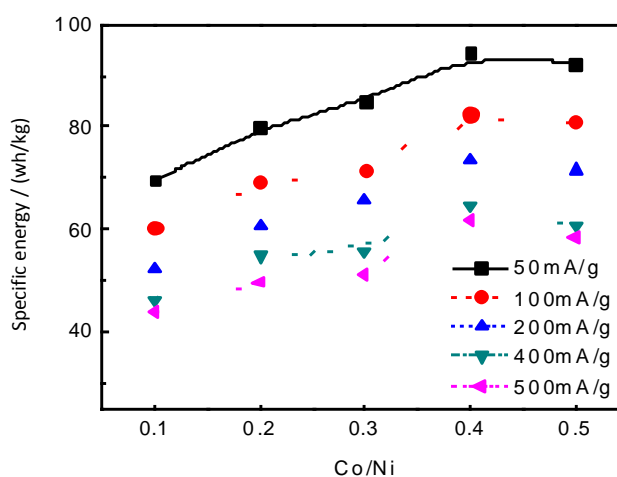


Figure 4. Capacitive property curves of Co-doped NiO material.

In Fig.4, it indicated that the specific energy of Co-doped NiO could be enhanced with the increase of the Co content, which achieved maximum at the Co/Ni molar ratio of 0.4. It could be attributed to the increase of the conductivity and the capacity of NiO after the doping of Co due to the pseudocapacitance performance of CoO. Meanwhile, some Co could be inserted into the lattice of the Ni oxide, which improved the ion transportation between NiO grains, reducing resistance and improve the capacity of supercapacitor[18]. However, the specific energy would reduce partly if the Co content

continues to rise, a specific energy of $61.67 \text{ wh}\cdot\text{kg}^{-1}$ under the current density of $200 \text{ mA}\cdot\text{g}^{-1}$, as indicated in Fig.4.

3.5 Self-discharging performance of Co-doped NiO material

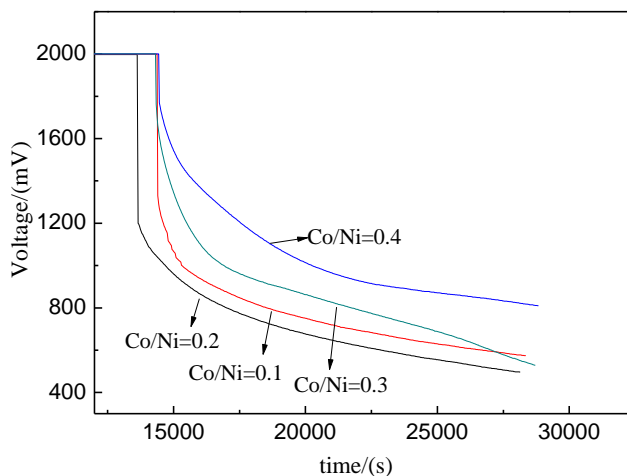


Figure 5. Self-discharging curves of Co-doped NiO material

In Fig.5, it was shown that the Co-doped NiO electrode at the Co/No molar ratio of 0.2 had the maximum instant potential drop at the onset of discharging, which could be ascribed to the high current at the local area of electrode surface resulted from the non-uniform coatings on electrodes.

The NiO showed the lowest potential drop at the doping ratio of Co/Ni of 0.4, because the conductivity was increased and the internal resistance was reduced after Co^{2+} doping. In the potential range of 1.6V-0.9V, the discharging curves exhibited an exponential relationship with time, which indicated self-discharging of a electric double layer existed in these materials. The electric double layer at the interface of electrode/solution consisted of a compact layer and a diffusion layer. The ion concentration of solution outside the diffusion layer was homogeneous. During the charging process, the ions moved toward the electrode surface and entered into the electric double layer under the action of electric field, which contributed to the ion concentration gradient in the diffusion layer[19]. Furthermore, the voltage consisted of diffusion layer potential and electric double layer potential at this stage. After charging process, the ions in the diffusion layer moved quickly toward the bulk solution, which led to the sharp drop of capacitor voltage until the diffusion layer potential approached 0 V. At last, the impurity discharging existed in the electrode material.

3.6 Cycle performance of Co-doped NiO material

In Fig.6, it showed that the capacity decreased slightly with the increase of cycling times. The cycle performance of Co-doped NiO improved while the Co content increase. Moreover, the doping ratio of Co/Ni of 0.4 displayed the highest capacity performance. The capacity attenuation after 500 cycles was listed in Table 1. Given that the capacity of pure NiO was attenuated by 12% after 100

cycles, the obvious enhancement of cycle performance of modified NiO could be resulted from the substitute of Ni by Co in the lattice to form cation defects. Hence, the doped NiO conductivity and cycling performance were increased and the electron resistance was reduced.

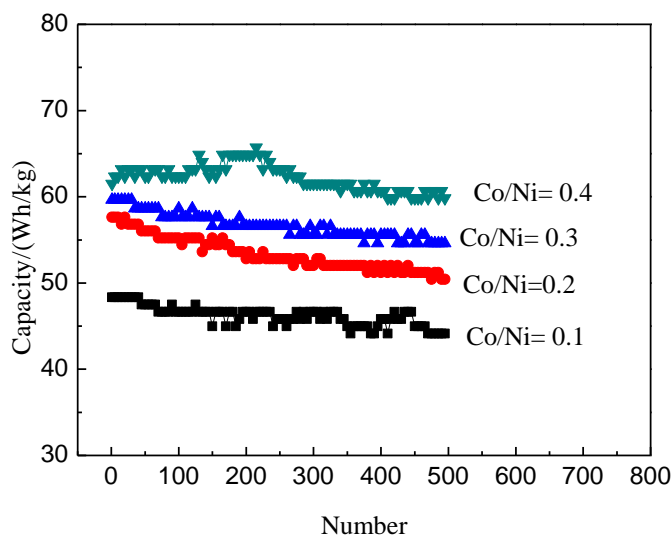


Figure 6. Cycle performance of Co-doped NiO

Table 1. Attenuation of capacity of Co-doped NiO after 500 cycles

Co/ Ni (mol)	0.1	0.2	0.3	0.4
attenuated %	8.71%	12.5%	8.47%	7.79%

3.7 AC impedance analysis of Co-doped NiO

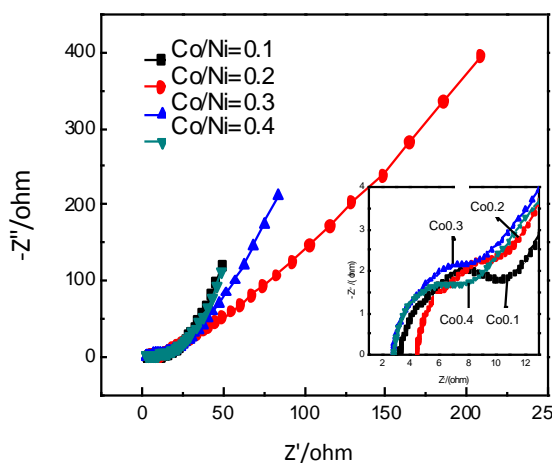


Figure 7. AC impedance spectra of Co-doped NiO

In Fig.7, the semi-circle shape of AC impedance curve in high frequency represented the chemical reaction resistance while the straight line shape in low frequency meant the diffusion

resistance. The more Co was doped the smaller the semi-circle diameter was. The chemical reaction resistance decreased correspondingly and reached a minimum at the ratio of Co/Ni of 0.4 due to the good conductivity of CoO. As the Co content increased, the conductivity of $\text{Co}_x\text{Ni}_y\text{O}$ electrode material was improved and resistance reduced, which indicated that the reaction take place more easily and quickly. The equivalent series resistance was highest at the ratio of Co/Ni of 0.2 while others were of little difference. The possible reason was the poor contact between active substance and current collector during the assembling, which increased the contact resistance, in essence, the equivalent series resistance.

3.8 Cyclic voltammetry analysis of Co-doped NiO

The CV curves of Co-doped NiO in the voltage ranging from -2V to -0.5V was displayed in Fig.8a, which indicated small area of CV curves and limitation of energy storage. From -0.5V to 1.5V, the induced current from CV curves became relative larger. The whole cyclic voltammetry curve shapes were center symmetry with a twisted rectangle. The induced current of modified NiO with the ratio of Co/Ni of 0.3 rised sharply at 1.5V, indicating an irreversible reaction occurred. In Fig. 8(b), it was observed that the induced current elevated with rising of the scan rate between -0.5V and 1.5V. When the scan rate got up to 100 mV/s, the CV curves were seriously distorted because of polarization.

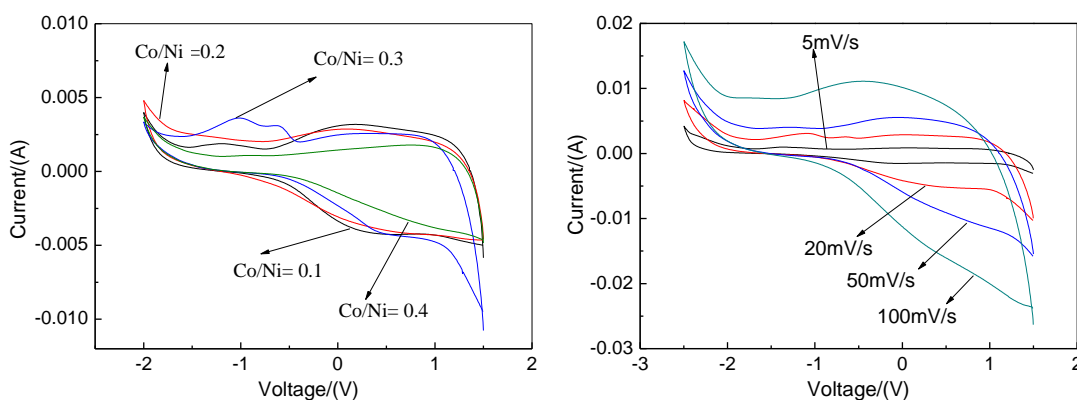


Figure 8. CV curves of Co-doped NiO (a) at different Co doping content at 20mV/s and (b) at different scan rate at the ratio of Co/Ni of 0.4

3.9 Capacity mechanism of Ni-based material

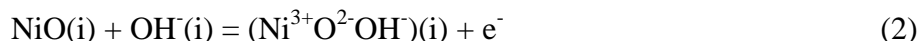
The formation of $\text{Ni}(\text{OH})_2$ involving in supercapacitors was realized through the transportation of electron defects and proton defects in the lattice of semiconductors. During the charging process, one H^+ from OH^- around Ni^{2+} moved out and one O^{2-} produced. Meanwhile, Ni^{2+} losed an electron and transformed to Ni^{3+} , turning $\text{Ni}(\text{OH})_2$ to NiOOH [20], as shown in Equation (1).



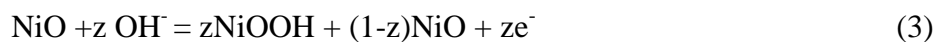
When Ni(OH)₂ and active carbon matched to form a mixed capacitor system, the system exhibited the capacity property.

This illuminated that Ni(OH)₂ could reserve electricity via electrochemical reactions in the capacitor system. Firstly, the reactions occurred on the surface of electrode materials. And then H⁺ resulted from the reaction diffused continuously toward the electrode surface, the reaction occurred at the interior of electrodes, which was consistent with Tian and Conway's conclusion.

For the modified NiO materials obtained by various treatments of Ni(OH)₂, the electrode reaction took place at the interface of NiO electrode/electrolyte solution firstly. It was considered that the capacity working mechanism was charge storage of surface electrochemical adsorption/desorption OH⁻, [21-22] as given in Equation (2).



In the above equation, "i" indicates the interface active reaction sites. Different from the reaction mechanism of Ni(OH)₂, the NiO electrode material could not form hydrogen bonds effectively due to the lack of free hydroxide radicals. The movement of OH⁻ was confined in the three-dimensional structure, which made the reaction localize on the surface, i.e., the surface reaction mechanism.



When the redox reaction took place between Ni²⁺ and Ni³⁺, only a portion of Ni atoms on the surface NiO particles involved in the reaction with a small z value, as shown in Equation (3). Thus, the key factor of improving the specific capacity of NiO electrode material was to reduce the particles' size and increase the specific surface area of NiO particles in order to raise the percentage of Ni atoms on the NiO crystal surface.



Moreover, electric double layer capacitor could also be formed by the charge confront derives from the oriented Li⁺ and ClO₄⁻ at the interface of NiO electrode/electrolyte solution. Li⁺ would enter into the lattice of NiO due to the poor crystallinity of NiO with abundant lattice defects under low treatment temperature. When the quasi-2D space on the electrode surface was embedded with Li⁺, the other Li⁺ and ClO₄⁻ would aggregate at the electrode surface and then form electric double layer capacitors. As the temperature of heating treatment rose, the crystal structure of NiO became perfect with few lattice defects, which meant that the quasi-2D space would be compressed after embedding of Li⁺. Meanwhile, the surface area of double layer charge reduced, which implied the decrease of the effective surface area involving the reaction. In other words, the capacity declined as the temperature elevated.

4. CONCLUSIONS

The asymmetric electrochemical capacitor can be configured using Co-doped NiO composite thin film as cathode material by microwave assisted modification and active carbon as anode material. Through cyclic performance and AC impedance tests, it was showed that Co_xNi_yO nano-composite thin film as electrode material had low resistance, long longevity and high capacity. The electrode

material with the Co/Ni=0.4 had the best performance: specific surface area of $146.21 \text{ m}^2 \cdot \text{g}^{-1}$, a specific energy of $61.67 \text{ wh} \cdot \text{kg}^{-1}$ under the current density of $200 \text{ mA} \cdot \text{g}^{-1}$ and an attenuation by 7.79% after 500 cycles, which demonstrated that the Co-doped NiO composite thin film would have significant potential as the electrochemical capacitor.

References

1. K. Liang, A. Chen, Z. S. Feng, *Acts Phys.-Chim. Sin.* 18 (2002) 383.
2. D. Liu, J. Shen, Y. J. Li, N. P. Liu, B. Liu, *Acta Phys. -Chim. Sin.*, 28(2012) 843
3. H. Wang, Z. Y. Tang, J. X. Li, *J. Solid State Electrochem.* 14(2010) 1525.
4. B. E. Conway, W. G. Pell, *J. Solid State Electrochem.* 9(2003) 637
5. B. Andrew, *J. Power Sources*, 91(2001) 37
6. D. H. Ftitts, *J. Electrochem. Soc.* 144(1997) 2233
7. S. Sarangapani, V. Tilakb, C. P. Chen, *J. Electrochem. Soc.* 143(1996) 3791
8. E. Z. Charl, A. Rory, J. Pynenburg, *J. Electrochem. Soc.* 145(1998) L61
9. X.Y. Wang, W. G. Huang, *J. Power Sources* 140(2005) 211
10. K. C. Liu, M. A. Anderson, *J. Electrochem. Soc.* 143(1996) 124
11. X. M. Liu, X. G. Zhang, S. Y. Fu, *Mater. Res. Bull.* 41(2006) 620
12. W. N. Kyung, B. K. Kwang, *J. Electrochem. Soc.* 149(2002) A346
13. X. M. Liu, X. G. Zhang, *Electrochim. Acta.* 49(2004) 229
14. H. Seiji, T. Hiromori *J. Power Sources* 194(2009) 1213
15. B. Gao, C. Z. Yuan, L. H. Su, S. G. Chen, X. G. Zhang, *Electrochim. Acta*, 54(2009) 3561
16. Q. H. Huang, X. Y. Wang, J. Li, C. L. Dai, S. Gamboa, P. J. Sebastian, *J. Power Sources* 164(2007) 425
17. M. Tian, B. E. Conway, *J. Electroanal. Chem.* 581(2005) 182
18. J.H. Par, S. Kim, O.O. Park, J.M. Ko, *Appl. Phys. A.* 81 (2006) 593.
19. A. D. Su, X. Zhang, A. Rinaldi, S.T. Nguyen, H. H. Liuc, Z. b. Lei, L. Lu, H. M. Duong, *Chem. Phys. Lett.*, 561(2013) 68
20. V. Srinivasan, J. W. Weidner, *J. Electrochem. Soc.* 146(1999) 1650
21. B. Ren, M.Q. Fan, Q. Liu, J. Wang, D. L. Song, X. F. Bai, *Electrochim. Acta*, 92 (2013) 197
22. F.B. Zhang, Y.K. Zhou, H.L. L, *Mater. Chem. Phys.* 83 (2004) 260